

Erase and Restore: Simple, Accurate and Resilient Detection of L_2 Adversarial Examples

Fei Zuo
University of South Carolina
fzuo@email.sc.edu

Qiang Zeng
University of South Carolina
Zeng1@cse.sc.edu

Abstract—By adding carefully crafted perturbations to input images, adversarial examples (AEs) can be generated to mislead neural-network-based image classifiers. L_2 adversarial perturbations by Carlini and Wagner (CW) are regarded as among the most effective attacks. While many countermeasures against AEs have been proposed, detection of adaptive CW L_2 AEs has been very inaccurate. Our observation is that those deliberately altered pixels in an L_2 AE, altogether, exert their malicious influence. By randomly erasing some pixels from an L_2 AE and then restoring it with an inpainting technique, such an AE, before and after the steps, tends to have different classification results, while a benign sample does *not* show this symptom. Based on this, we propose a novel AE detection technique, Erase and Restore (E&R), that exploits the limitation of L_2 attacks. On two popular image datasets, CIFAR-10 and ImageNet, our experiments show that the proposed technique is able to detect over 98% of the AEs generated by CW and other L_2 algorithms and has a very low false positive rate on benign images. Moreover, our approach demonstrate strong resilience to adaptive attacks. While adding noises and inpainting *each* have been well studied, by combining them together, we deliver a simple, accurate and resilient detection technique against adaptive L_2 AEs.

I. INTRODUCTION

By adding deliberately crafted perturbations into a normal image, an attacker is able to create an *adversarial example* (AE), which misleads a neural-network-based classifier to output an incorrect prediction result. Worse, the malicious perturbations in an AE are so subtle that they are usually human-imperceptible. As neural networks are increasingly deployed, AEs raise crucial security concerns especially in many vision-related applications.

To gauge such adversarial perturbations, L_p norms are usually used to quantitatively describe the discrepancy between an original benign image I_o and its corresponding AE I_a . According to the value of p , the mainstream AE generation algorithms can be categorized into three families: L_0 , L_2 and L_∞ attacks. Informally, L_0 measures the number of modified pixels, L_2 the Euclidean distance between the two images, and L_∞ the largest modification among all the modified pixels.

In particular, L_2 attacks by Carlini and Wagner (CW) [6] “are among the most effective white-box attacks and should be used among the primary attacks to evaluate potential defences”[29]. Although researchers have proposed many AE detection methods [21], [27], [26], [37] to assist the protected neural networks in rejecting adversarial inputs, recent studies [19], [5], [4] show that the detection usually



(a) Original image (b) Corrupted image (c) Restored image
Fig. 1: Restoring lost parts of an image with inpainting.

goes ineffective when facing adaptive CW L_2 AEs. How to accurately detect adaptive L_2 AEs is still an unresolved challenge. Thus, we focus on tackling L_2 AEs in this work, and our goal is a technique that not only detects L_2 AEs but is also resilient to adaptive attacks.

We have two key insights. First, we observe that those deliberately corrupted pixels exert a malicious influence *as a whole*. It implies that a destruction of the completeness of the influence by all perturbed pixels may cause a failure of the attack. Second, although destruction may also harm the classification accuracy for benign samples, there exist very effective *inpainting* techniques [34], [35], [25] in the image processing area that can help restore a partially corrupted image. For example, Figure 1(a) shows an original image. Figure 1(b) presents a corresponding corrupted image where many regions are erased. After inpainting, as shown in Figure 1(c) the corrupted image is well restored.

Thus, we hypothesize that if we *randomly* erase quite a few pixels from an AE and then apply inpainting to the resulting AE, the AE attack will probably fail for two reasons. First, discarding many small regions from an AE will ruin the holistic adversarial influence formed by the maliciously perturbed pixels. Second, the inpainting typically restores the image in a benign way that does *not* uphold the malicious influence. By contrast, if we apply the same “Erase-and-Restore” (E&R) operations to a benign sample, the classification results, before and after the steps, tend to be identical, as inpainting by design is supposed to reverse the deterioration to benign images.

Figure 2 illustrates our insights and observations using six color images from CIFAR-10. A *random mask* (mask, for short) in our work describes the locations of pixels that are randomly erased. We randomly erase 5% of the pixels of each image. The AEs are generated using the CW algorithm

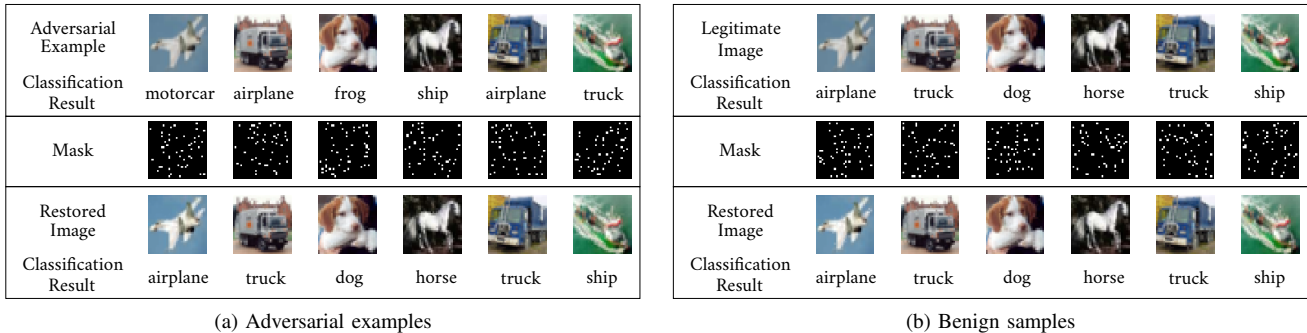


Fig. 2: Different impacts of the ‘‘Erase-and-Restore’’ (E&R) operations on AEs and benign samples.

(Section 2). As shown in Figure 2(a), the classification results of each AE, before and after the E&R operations, are different. By contrast, as shown in Figure 2(b), the classification results of each benign sample, before and after the steps, are the same. Our large-scale experiments also show consistent results (Section 4).

We consider the sensitivity to E&R operations as an exploitable characteristic of L_2 AEs. Based on this, we propose a very simple AE detection approach: given an image, if the classification results before and after E&R vary, it is an AE; otherwise, a benign sample. We accordingly implement an AE detector, named THEMIS, to thwart attacks created by state-of-the-art L_2 AE generation techniques. Our proposed detector applies the E&R operations to inputs, and is further enhanced by the idea of generating multiple samples. Specifically, given an image I_0 , we generate n images by *randomly* erasing some pixels of I_0 each time, to create a sequence of images $\{I_1, I_2, \dots, I_n\}$. For each deteriorated image, the locations of the erased pixels are described in a mask. Next, an inpainting technique is leveraged to restore the erased pixels based on masks and obtain the restored images $\{I'_1, I'_2, \dots, I'_n\}$. Finally, a classifier makes use of the prediction result of I_0 and those of the restored images to determine whether I_0 is an AE.

We have evaluated our system using the popular image datasets CIFAR-10 and ImageNet. While both leading L_2 AE generation methods, CW [6] and DeepFool [28], are considered in the evaluation, we lay special emphasis on CW [6] because it can circumvent all existing detectors, especially when adaptive attacks are considered. Our experiments show that the proposed detection technique is very effective. Take the CW [6] attack as an example, on the CIFAR-10 dataset, THEMIS can detect 99.8% AEs with a false positive rate (FPR)=0, and on ImageNet, it can detect 98.4% AEs with $FPR = 1.4\%$. More importantly, it shows high resilience to adaptive attacks.¹ The key contributions of our work include:

- We identify an interesting characteristic of L_2 AEs, whose classification results vary sharply when erasing and restoring operations are applied. Meanwhile, benign samples are not so sensitive. We exploit this distinction

and propose a simple but very effective approach—‘‘Erase and Restore’’—to detecting AEs.

- We employ the idea of sampling to enhance the proposed detection approach. By applying E&R to an input for multiple times, richer features are generated to improve the detection accuracy. Moreover, for each sample, the erased pixels are randomly selected, which makes the approach highly unpredictable from the perspective of attackers.
- We implement this approach in our detector THEMIS and evaluate it on two popular datasets, CIFAR-10 and ImageNet. The experiment results show that THEMIS outperforms prior techniques and achieves the highest detection accuracy.
- The enormous randomness and the non-differentiable nature are inherent strengths of our detection approach, which make it difficult for an adversary to circumvent THEMIS. The evaluation results corroborate that our system is highly resilient to adaptive attacks.

The rest of the paper is organized as follows. We introduce some background and the threat models in Section 2, and the experimental setup in Section 3. Section 4 describes our proposed approach. We present the evaluation results in Section 5. We evaluate the resilience of the proposed technique under adaptive attacks in Section 6. The related work is reviewed in Section 7. We discuss our work and draw conclusions in Section 8 and Section 9, respectively.

II. BACKGROUND AND THREAT MODELS

A. Attack Algorithms

Adversarial attacks can be categorized as either non-targeted or targeted ones. The aim of a non-targeted attack is to make the input be classified as any arbitrary class except the correct one. By contrast, the aim of a targeted attack is a specific attacker-desired, but actually incorrect, prediction result. Next, we briefly describe two leading L_2 AE generation methods.

1) *Carlini & Wagner Attacks*: Carlini and Wagner [6] designed a group of targeted AE generation methods which are denoted as CW attacks. According to the distance metrics adopted in an optimization target, CW attacks can be divided into three types: L_0 -, L_2 - and L_∞ -norm. In this paper, we

¹All the code and data in this paper will be open sourced.

mainly examine *CW* L_2 attacks, which are the most difficult to detect [19], [4].

Due to a few creative designs, the CW attacks achieve performance superior to other attack methods. The first and foremost innovative design is using a logits-based objective function rather than softmax-cross-entropy loss, which plays a key role in the resilience improvement of the attack against defensive distillation [30]. Secondly, this algorithm maps the target variable to a space of the inverse trigonometric function, so that the problem is suitable to be solved by a modern optimizer, e.g. Adam [20]. Finally, a *confidence-level* parameter κ is introduced; as κ increases, the model classifies the resulting AE as the attacker-desired label more likely, giving the attacker flexibility to make a trade-off between the degree of perturbations and misclassification probability.

2) *DeepFool*: Moosavi et al. [28] developed the DeepFool attack that is used to create non-targeted AEs. The algorithm utilizes an iterative linearization of the classifier to generate L_2 minimization-based perturbations. To simplify the problem, the neural networks are imagined to be linear, so that the decision boundaries are a set of hyper-planes. Consequently, a polyhedron can be used to describe the output space. Assuming that f is a binary differentiable classifier, to mislead the decision of f near the current point x_i , the minimal perturbation is the orthogonal projection of x_i onto the separating hyper-plane. At each iteration the minimal perturbation of the linearized classifier is computed as

$$\arg \min_{\delta_i} \|\delta_i\|_2 \quad \text{s.t.} \quad f(x_i) + \nabla f(x_i)^T r_i = 0 \quad (1)$$

where δ_i is the minimum perturbation imposed on x_i . Note that neural networks are not actually linear, so the searching will be repeated until a successful AE is found.

B. Threat Model: Adaptive Attacks

The adversary has not only full knowledge of the target model (including both its architecture and parameters), but also the existence and internal details of the detector, and can *adapt attacks accordingly*. In this scenario, the attacker tries to fool the neural-network-based classifier and the detector at the same time. We consider adaptive attacks and evaluate the resilience of our detector to them in Section VI.

III. EXPERIMENTAL SETUP

Before presenting our defense scheme, we introduce the image datasets and the corresponding target neural networks on which we verify our key insights and evaluate the proposed approach.

Image datasets. We generate AEs using two popular datasets: CIFAR-10 and ImageNet, both of which are widely used in image classification tasks. In particular, for ImageNet, we adopt the *ILSVRC2012* samples to keep consistent with the prior state-of-the-art AE detector [23].

Target neural network models. (1) For CIFAR-10, we use two neural networks as the target models: a 32-layered ResNet model [18] (denoted as *ResNet32*), and a model structure described in [6] (denoted as *Carlini*). We train

these two target neural network models from scratch, and their accuracies are 91.96% and 78.86%, respectively. (2) For ImageNet we re-use a 50-layered ResNet model [18] provided in Keras [7] (denoted as *ResNet50*).

AE generation. Only those images that are correctly classified by the corresponding target model are used to generate AEs used in our experiments. To generate the *targeted* AEs, we designate the *next* class as the target class, similar to many other AE detection works [23], [37], [39]. We only keep the AEs that can successfully fool the target models—that is, those perturbed images which fail to attack the corresponding target model directly are not considered in our evaluation. Moreover, all AEs are generated using the open-source tool `Foolbox` [33].

Inpainting algorithm. We adopt Telea’s inpainting algorithm [35] in our work. Since this inpainting algorithm needs to solve an *Eikonal* equation, which is rarely differentiable everywhere, the *fast marching* method is leveraged to find the solution based on a finite difference approximation. Thus, the inpainting algorithm adopted in our work is *not* fully differentiable, resulting in a non-negligible obstacle for adaptive attackers.

The experiments were performed on a computer equipped with an Intel® Core™ i9 CPU, 32 GB RAM and dual GeForce® GTX 1080 Ti GPU cards.

IV. THE PROPOSED APPROACH

A. Our Insights

Limitations of erasing (or adding noises) alone. Due to the optimization nature of AE generation methods like CW and DeepFool, maliciously manipulated pixels in an AE are deliberately selected and perturbed. Thus, each of the perturbed pixels plays a certain role in the attack. By *randomly erasing* many pixels of an input image, it is likely to corrupt some of the perturbed pixels or their surrounding pixels in an AE, rendering the attack ineffective.

In the case of *benign* samples, however, the erasing operation, which is equivalent to introducing random noises to images, will significantly degrade the accuracy of the classifier. The close correlation between the image quality and the accuracy of image classification has been widely studied in previous works [11], [9], [12]. They mention that neural networks are susceptible to random noise distortions. For example, Costa et al. [9] point out that “*noises can hinder classification performance considerably and make classes harder to separate.*”

Combining erasing and inpainting. We thus propose to apply *inpainting* after the erasing operation. Inpainting is a category of techniques for restoring damaged regions of images. Given an erased region, an inpainting technique infers and recovers its original pixels. *Our insight* is that while inpainting works very well for recovering benign samples, its recovering effect usually is *not* what the AE attacker desires, since the maliciously perturbed regions, once erased, can hardly be recovered to the attacker-intended values.

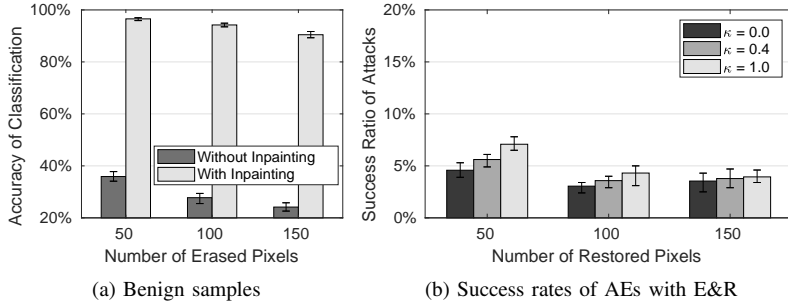


Fig. 3: Impacts of E&R on benign samples and AEs.

We further design experiments to verify the two insights in Section IV-B.

B. Verifying Our Insights

From CIFAR-10, we randomly select 1,000 images that can be correctly classified by *ResNet32*. As shown in Figure 3(a), after randomly erasing 50~150 (around 5%~15%) of the pixels in each image, without inpainting, the classification accuracy significantly degrades from 100% to the range from 24.2% (when erasing 15%) to 35.9% (when erasing 5%), which verifies that erasing alone harms the classification accuracy for benign images significantly. By contrast, with inpainting applied, the classification accuracy recovers to the range from 90.5% to 96.6%.

Besides, we use the CW algorithm to generate three AEs for each benign image with three different confidence levels ($\kappa = 0.0, 0.4, \text{ and } 1.0$, respectively). All the AEs successfully fool the *ResNet32* model. As shown in Figure 3(b), after randomly erasing 50~150 (around 5%~15%) of the pixels in each AE and then restoring them using inpainting, the success rate of attacks dramatically decreases from the original 100% to the range from 3.1% to 7.1%.

Similar results can be observed on the ImageNet dataset as well. (1) Specifically, we randomly select 1,000 images from ImageNet that can be correctly classified by the *ResNet50* model. For example, after erasing and restoring 5% of the pixels in each image, the classification accuracy stays at 96.3%. (2) On the other hand, when we apply the same erasing and restoring operations to the 1,000 AEs generated from these benign images, the success rate of attacks decreases from 100% to around 4.1%.

Therefore, it can be concluded that E&R has very small impacts on benign samples, but has much larger impacts on AEs, demonstrating a noticeable distinction.

C. Approach Details

Based on our insights, we propose a novel AE detection approach, named E&R, that exploits such a distinction and implement it in a prototype system, called THEMIS, as shown in Figure 4. (1) Given an input image I_0 , we **randomly erase** λ **pixels** of it to create a deteriorated image I . This step is repeated for n times to obtain a sequence of deteriorated images $\{I_1, I_2, \dots, I_n\}$, using the idea of sampling. The *intuition* behind it is that even if an AE “luckily” evades the detection once, it is very unlikely for it to hide itself

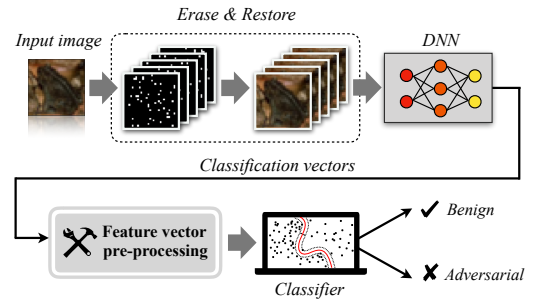
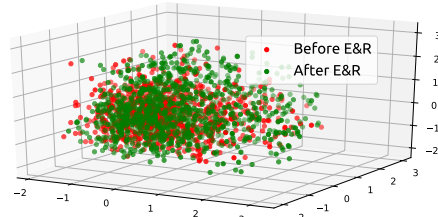
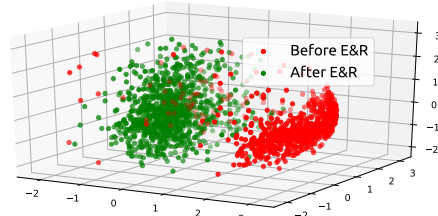


Fig. 4: Architecture of THEMIS.



(a) Benign samples



(b) AEs

Fig. 5: Visualization of feature vectors.

throughout the multiple samples. (2) Next, an inpainting technique is leveraged to produce a corresponding sequence of **restored** images $\{I'_1, I'_2, \dots, I'_n\}$. (3) Finally, we feed both the input image I_0 and the sequence of restored images $\{I'_1, I'_2, \dots, I'_n\}$ into a target neural network, and collect all the classification results.

Given an image in CIFAR-10, its classification result is a vector $\in \mathbb{R}^{10}$ (since there are 10 classes in the dataset). We simply concatenate all the classification-result vectors for both I_0 and $\{I'_1, I'_2, \dots, I'_n\}$ to obtain a feature vector $\in \mathbb{R}^{10 \times (n+1)}$ for training the AE classifier.

Given an image from the ImageNet, its classification result is a vector $\in \mathbb{R}^{1000}$ (since there are 1,000 classes in the dataset). Thus, the number of features to be fed to our classifier is $1000 \times (n+1)$, which is too large. To make the training of our classifier more feasible, Principal Component Analysis (PCA) is performed on the classification results of I_0 and $\{I'_1, I'_2, \dots, I'_n\}$, to reduce the dimensionality to a lower value d . Unless otherwise specified, we set d to 10 (1% of the original dimensionality) to keep consistent with CIFAR-10. Note that the number of principal components should be less than both the number of features and the number of samples, when solving PCA based on the truncated SVD (singular value decomposition). In our case, the number of samples is $n+1$; we thus let $n=11$ (we discuss the impact

TABLE I: Performance of THEMIS. Cells with shading are results using *SVM*, and cells without shading *AdaBoost*.

Dataset	Target Model	FPR	Detection Rate		
			$\kappa=0.0$	$\kappa=0.4$	$\kappa=1.0$
CIFAR-10	Carlini	0.4%	100%	100%	100%
		0.0%	99.8%	99.9%	99.7%
	ResNet32	2.8%	99.6%	99.7%	99.7%
		0.8%	99.0%	99.2%	98.9%
ImageNet	ResNet50	3.2%	97.6%	98.1%	98.5%
		1.4%	98.4%	98.5%	98.9%

of n 's values with detailed experimental results in Section V-C). We concatenate the vectors of principal components for both I_0 and $\{I'_1, I'_2, \dots, I'_n\}$ to obtain a feature vector for training our classifier.

We train our AE classifier using two supervised learning techniques: *AdaBoost* [13] and *SVM* [8] with the RBF (radial basis function) kernel.

The value of the parameter λ is set to 10% of the pixels in our implementation. We adopt this value for two reasons. (1) As shown in Figure 3, when 10% of the pixels are erased and restored, it harms the success rate of AEs most heavily, without degrading the classification accuracy for benign samples significantly. (2) The inpainting algorithm we adopt performs very well when the portion of corrupted pixels in an image is less than 15% [35].

It is worth mentioning that $\lambda = 10\%$ leads to an enormous randomness pool. Take an image in CIFAR-10 as an example, the size of which is 32×32 . With $\lambda=100$ ($\approx 10\%$ of the pixels), the number of unique masks is around 7.7×10^{140} . It is thus very unlikely for an attacker to correctly predict which mask is used.

Visualization of feature vectors. The feature vectors due to 1,000 benign samples from the ImageNet dataset and the corresponding 1,000 AEs are visualized in Figure 5, which shows only three principal components. We have two observations. (1) While the feature vectors of benign samples, before and after the E&R operations, are close (Figure 5(a)), those of AEs, before and after the same operations, form two clusters far apart (Figure 5(b)). This is consistent with our experiments shown in Figure 3 and verifies our insights once again. (2) PCA is effective in preserving features that help distinguish benign samples from AEs.

V. EVALUATION

A. Performance Under CW Attacks

To train the detector, we firstly prepare datasets including negative (i.e., benign samples) instances from CIFAR-10 and ImageNet and positive ones (i.e., AEs). For each target model, we adopt the CW L_2 algorithm to generate AEs; and for each confidence level (i.e., $\kappa = 0.0, 0.4, \text{ and } 1.0$), we generate 5,000 *successful* AEs. Accordingly, we prepare 15,000 benign images which all can be correctly classified. In the dataset, 80% of instances are used for training, and the remaining 20% are used for testing.

We evaluate the performance of THEMIS in terms of *detection rate* and *false positive rate* (FPR). The detection rate is defined as the ratio of the number of successfully detected AEs to the total number of AEs. FPR refers to the fraction of the negative testing data (i.e., benign samples) that is misclassified as positive (i.e., AEs). As shown in Table I, the proposed technique achieves very high detection rates (up to 100% on CIFAR-10, and 98.9% on ImageNet) with low FPR values. The results are stable across different target models, confidence levels, and classification methods.

Comparison with the prior work. We compare THEMIS with the state-of-the-art AE detector—NIC [23]. Their experiments only examine $\kappa = 0.0$, which is the default setting. With respect to CIFAR-10, NIC considers the *Carlini* target model and obtains the detection rate 96% and FPR 4.2% (see Table I in [23]), while our system achieves the detection rate **99.8%** and FPR **0%**. With respect to ImageNet, NIC considers the *ResNet50* model and its detection rate is 96% with FPR=14.6% (see Table I in [23]), while our detection rate is **98.4%** with FPR=**1.4%**. It is worth noting that the distribution of adversarial and benign images is not balanced in practice—most inputs should be benign. Thus, FPR is a very important metric to evaluate the model performance: a lower FPR indicates that the system makes fewer mistakes for benign images. THEMIS is able to keep both a high detection rate and a *very low FPR*.²

Target-model agnostic. We are interested in finding out whether a detector trained using AEs targeting one model can be directly used to detect AEs targeting another—that is, whether it is *target-model agnostic*. We thus train our system using AEs that target the *Carlini* model, and test it using AEs that target *ResNet32*. As Table II shows, the detection rate is as high as 100%. We then train the system using AEs that target *ResNet32*, and test it using AEs that target *Carlini*; the detection rate is as high as 99.9%. These results are based on images from CIFAR-10. And, the experimental results based on ImageNet are similar. Therefore, this experiment not only confirms that THEMIS is *target-model agnostic*, but also demonstrates that THEMIS has low risk of overfitting.

B. Performance Under DeepFool Attacks

While our focus is CW L_2 attacks, we also seek to understand whether the proposed technique is effective in detecting L_2 AEs generated using another leading algorithm—DeepFool (see Section II-A.2). We use CIFAR-10 in this experiment as a showcase. For each target model (*ResNet32* and *Carlini*), 15,000 *successful* AEs and the corresponding benign samples are prepared. We use 80% of the data to train the detector and 20% to test the detector.

Table III shows the experimental results. Given the *Carlini* model, our system obtains the detection rate **99.1%** and FPR **0.4%**, while NIC [23] obtains the detection rate 91.0% and FPR 4.2% (see Table I in [23]). Thus, the performance of

²We intended to compare with [36] as well, which depicts the results in a figure (Figure 6 in [36]). We wrote emails to the authors asking for numeric results, but have not received responses up until the submission.

TABLE II: Target-model agnostic property of THEMIS.

Target Model (Train → Test)	Classifier	Detection Rate		
		$\kappa=0.0$	$\kappa=0.4$	$\kappa=1.0$
Carlini→ResNet32	SVM	100%	100%	100%
	AdaBoost	97.9%	97.9%	98.2%
ResNet32→Carlini	SVM	99.9%	99.9%	99.8%
	AdaBoost	99.7%	99.8%	99.6%

TABLE III: Performance of THEMIS evaluated on DeepFool.

Target	Classifier	FPR	Detection Rate
Carlini	SVM	0.4%	99.1%
	AdaBoost	0.2%	98.1%
ResNet32	SVM	4.0%	99.5%
	AdaBoost	1.6%	99.6%

TABLE IV: Impacts of different values of n . Cells with shading are results using SVM, and cells without shading AdaBoost.

Dataset	Target Model	$n = 3$				$n = 5$				$n = 7$			
		FPR	Detection Rate			FPR	Detection Rate			FPR	Detection Rate		
			$\kappa=0.0$	$\kappa=0.4$	$\kappa=1.0$		$\kappa=0.0$	$\kappa=0.4$	$\kappa=1.0$		$\kappa=0.0$	$\kappa=0.4$	$\kappa=1.0$
CIFAR-10	Carlini	0.4%	100%	100%	100%	0.4%	100%	100%	100%	0.4%	100%	100%	100%
		0.0%	100%	100%	99.9%	0.0%	100%	99.9%	99.9%	0.0%	100%	100%	99.8%
	ResNet32	3.6%	99.6%	99.6%	99.6%	3.3%	99.6%	99.6%	99.6%	2.9%	99.6%	99.7%	99.7%
		0.9%	99.2%	99.1%	98.5%	0.7%	99.2%	99.1%	99.0%	0.9%	99.3%	99.1%	98.9%
ImageNet	ResNet50	9.8%	95.4%	95.1%	95.5%	4.7%	95.5%	95.8%	97.3%	3.6%	97.6%	98.1%	98.2%
		6.6%	93.1%	91.4%	93.8%	2.8%	96.5%	97.6%	97.2%	2.1%	97.9%	98.6%	98.6%

our system is significantly better than NIC. For the *ResNet32* model, our system has the detection rate 99.6% with FPR = 1.6%; however, NIC did not consider *ResNet32*.

Transferability. We are also interested in the transferability of our detector—whether THEMIS trained on one type of AEs can be directly applied to detect another type of AEs that are *unseen* during training. To verify it, we *train* THEMIS using CW AEs with mixed confidence levels. Without loss of generality, in the process of CW AE generation, we only use *Carlini* as the target model. We test the trained system using DeepFool AEs targeting *ResNet32* and DeepFool AEs targeting *Carlini*, and our system can achieve detection rates 97.1% and 96.2%, respectively. Thus, we can conclude the proposed technique has very good transferability, that is, it keeps effective in handling unseen AE generation methods.

Explanation. The two notable properties of THEMIS—target-model agnostic and good transferability—can be attributed to the unique advantage of the proposed approach: regardless of the target model and the attack method, benign samples and AEs show distinct sensitivities to the E&R operations (see Section 4).

C. Value Selection for the Parameter n .

We use $n = 11$ in the previous experiments. Here, we investigate the impacts of different values of n on the detector’s performance. The results are shown in Table IV. To compare with the results in Table I, all the AEs are generated using the CW L_2 algorithm as well. For CIFAR-10, which has only 10 classes (thus no PCA is needed), varying the value of n has little impacts. However, for ImageNet, the value of n has noticeable impacts: when n increases, the AE detection rate increases and FPR decreases. The reason is that by increasing n , more principal components can be extracted (see Section 4). However, when $n > 11$, the performance improvement is negligible, probably because the extra principal components do not provide useful features for AE detection. Therefore, we adopt $n = 11$.

VI. RESILIENCE TO ADAPTIVE ATTACKS

In an adaptive attack threat model, an adversary knows the existence and internal details of our detector and *adapts* the attacks to bypass the detection. We thus seek to study the resilience of THEMIS to adaptive attacks.

An AE detector can be categorized as either differentiable or non-differentiable. Several previous works propose defense mechanisms that apply differentiable transformations to an image before detection or classification [27], [14], [15], [36]. But attackers can circumvent these differentiable defenses by “differentiating through them”—*i.e.*, by taking the gradient of a class probability regarding input pixels through both the CNN and the transformation [31], [4], [19]. This strategy, however, is *inapplicable* to bypassing THEMIS. Due to the random-erasing and inpainting-based restoring, our approach is not only non-differentiable but involves tremendous randomness.

To bypass non-differentiable defences, Backward Pass Differentiable Approximation (BPDA) is proposed [1]. To handle defenses that employ randomized transformation to the input (like ours), it applies Expectation over Transformation [2] to compute the gradient over the expected transformation to the input. However, in our approach the erased pixels are randomly selected among all the image pixels, and there are around 7.7×10^{140} unique masks (even for a small image; see Section IV-C); thus, it is infeasible to calculate the expected transformation. Moreover, THEMIS is not only randomized but also non-differentiable; in this case, it is unknown how to apply BPDA to bypassing THEMIS.

He et al. [19] describe a representative adaptive attack method against non-differentiable defences, where an attacker tries to circumvent the defensive approach by (a) considering intermediate distorted images during optimization and (b) exploring multiple diverse optimization paths. Inspired by [19], we design similar adaptive attacks to examine the resilience of our approach.

Adaptive AE generation. To that end, we modify the code

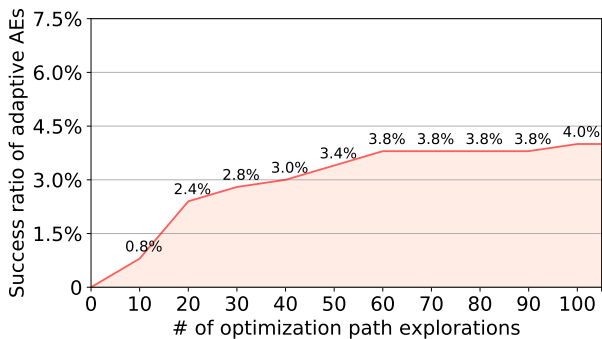


Fig. 6: Success ratio of adaptive AEs.

of the CW algorithm [6], in order to adaptively generate AEs that can bypass our detector. Specifically, after each iteration in an optimization procedure, an intermediate distorted image is obtained. We then check whether it can bypass our detector. For each image, we repeat the optimization procedure for up to T times to explore different optimization paths (for this purpose, we set a randomly initialized state at the beginning of each optimization procedure). We set $T = 100$, corresponding to around 300 seconds on average on our machine. In comparison, the two works [36] and [19] use around 75 and 180 seconds to generate adaptive AEs for each image, respectively.

Given that adaptive CW AE generation is quite time-consuming, without loss of generality, this experiment is conducted on 500 images randomly selected from CIFAR-10. During the AE generation, we let $\kappa = 0.0$, which means that the resulting AE is classified as the target class. As κ increases, the model classifies the resulting AE as the attacker-desired label more likely. As a larger value of κ imposes an extra constraint to attackers and lowers the chance of successful adaptive attacks, we only consider $\kappa = 0.0$.

Resilience results. We adopt the SVM-based detector, which achieves a detection rate of 100% (Table I). This means that no AEs can fool it *without adaptive attacks*.

Figure 6 shows that only 4% (that is, 20 AEs) of adaptive AEs can bypass our detector. By contrast, similar adaptive attacks [19] can bypass *feature squeezing* based AE detection [37] at a success rate of 100%. More importantly, the first 50 times of the optimization path exploration attain the success rate of 3.4%, while the second 50 times only increase the success rate by 0.6%. It shows that the effect of adaptive attacks grows very slowly as the attacker doubles his time. We thus can conclude that our detection approach is not only resilient to adaptive attacks based on differentiation-based attack methods, but also difficult to bypass through exploring many optimization paths.

VII. RELATED WORK

Countermeasures against AE attacks can be roughly divided into two categories. The first category aims to eliminate the influences of AEs by either rectifying them or fortifying the target neural network itself. The second category is AE

detectors like our work. Given the large body of research on AEs, this is not intended to be exhaustive.

A. Adversarial Influences Elimination

Adversarial training augments the training set with the label-corrected AEs [38], [24]. Buckman et al. [3] propose using thermometer-encoded inputs to assist adversarial training. Alternatively, *Shield* [10] enhances a model by re-training it with multiple levels of compressed images using JPEG, a commonly used image compression technique.

Another strategy is to pre-process the inputs before feeding them to neural networks. For instance, the pixel deflection and a wavelet-based denoiser are combined to rectify AEs [31]. Liao et al. [22] propose higher-level guided denoisers aiming to remove the adversarial noise from inputs. Some other methods adopt JPEG compression techniques [32], [16] to filter out the information redundancy, which otherwise provides living space for adversarial perturbations. However, their accuracies under adaptive attacks are lack of adequate evaluations. CIIDefence [17] proposes to use image inpainting with wavelet based image denoising to rectify the classification result. However, its inpainting mask is guided by class activation maps which might be predicted and exploited by an adaptive attacker.

B. Adversarial Examples Detection

Li et al. [21] extract PCA features after inner convolutional layers of the DNN, and then use a cascade classifier to detect AEs. Metzen et al. [27] train a CNN-based auxiliary network. This light-weight sub-network works with the target model to detect AEs. Some techniques apply pre-processors on input images and use prediction mismatch strategy to detect AEs. For example, Meng et al. [26] train an auto-encoder as the image filter. If the predictions of an original image and the corresponding processed one fail to match, the input is adversarial. Similarly, Xu et al. [37] propose *feature squeezing* to detect AEs by comparing the prediction for the original input with that for the squeezed one. However, adaptive attacks have successfully circumvented all of the aforementioned detection methods [4], [5], [19].

Finally, Tian et al. [36] leverage image rotation and shifting as pre-processors to construct a detector. Although these operations can produce certain randomness to counter some adaptive attacks, their randomness pool is very limited. It only has 45 possible transformations. As a result, their method can merely achieve a detection ratio of 70% under adaptive attacks [36].

VIII. DISCUSSION AND LIMITATIONS

The proposed erasing and restoring approach works by destruction of the carefully perturbed pixels. Attackers thus may consider minimizing the number of perturbed pixels in order to evade our detection. However, the prior work [39] points out that L_0 AE generation results in large amplitudes of altered pixels, which can be exploited to locate and restore most of the maliciously perturbed pixels. Therefore, how to make a trade-off between the number of altered pixels and

TABLE V: Performance of integrating THEMIS with an existing detector [39].

Classifier	FPR	Detection Rate			
		CW- L_0	JSMA	CW- L_2	DFool
SVM	4.5%	98.8%	99.6%	97.2%	98.0%
AdaBoost	2.6%	98.8%	99.6%	96.4%	97.2%

their resulting amplitudes is an interesting direction that is worth exploration for the AE generation purpose.

While our work focuses on detecting L_2 AEs, it is easy to combine our approach with other detectors that show strengths in detecting other types of AEs, in order to build a comprehensive hybrid detector; that is, an input is detected as an AE if any of the integrated detectors reports so. To illustrate this, as an example, we integrate our approach with the detection approach proposed in [39] to build a new and more universal detector that work for four different attacks, including CW- L_0 , JSMA, CW- L_2 , and DeepFool. Table V shows the performance of this hybrid detector.

IX. CONCLUSION

We have presented and verified our insight that L_2 AEs are sensitive to the erasing and restoring operations, while benign samples are *not*. Exploiting this insight, we have proposed a simple but very effective AE detection approach E&R. It outperforms other state-of-the-art approaches regarding both detection accuracies and FPR. Moreover, our detector is target-model agnostic, keeps effective across different attack methods, and is resilient to adaptive attacks.

REFERENCES

- [1] Anish Athalye, Nicholas Carlini, and David Wagner. Obfuscated gradients give a false sense of security: Circumventing defenses to adversarial examples. In *Proceedings of the 35th International Conference on Machine Learning, ICML 2018*, July 2018.
- [2] Anish Athalye, Logan Engstrom, Andrew Ilyas, and Kevin Kwok. Synthesizing robust adversarial examples. In *International Conference on Machine Learning*, pages 284–293, 2018.
- [3] Jacob Buckman, Aurko Roy, Colin Raffel, and Ian Goodfellow. Thermometer encoding: One hot way to resist adversarial examples. In *ICLR*, 2018.
- [4] Nicholas Carlini and David Wagner. Adversarial examples are not easily detected: Bypassing ten detection methods. In *ACM Workshop on Artificial Intelligence and Security*, 2017.
- [5] Nicholas Carlini and David Wagner. Magnet and “efficient defenses against adversarial attacks” are not robust to adversarial examples. *arXiv preprint arXiv:1711.08478*, 2017.
- [6] Nicholas Carlini and David Wagner. Towards evaluating the robustness of neural networks. In *IEEE Symposium on Security and Privacy (SP)*, 2017.
- [7] François Chollet. Keras. <https://keras.io>, 2015.
- [8] Corinna Cortes and Vladimir Vapnik. Support-vector networks. *Machine learning*, 20(3), 1995.
- [9] Gabriel B Paranhos da Costa, Welinton A Contato, Tiago S Nazare, João ES Neto, and Moacir Ponti. An empirical study on the effects of different types of noise in image classification tasks. *arXiv preprint arXiv:1609.02781*, 2016.
- [10] Nilaksh Das, Madhuri Shanbhogue, Shang-Tse Chen, Fred Hohman, Siwei Li, Li Chen, Michael E Kounavis, and Duen Horng Chau. Shield: Fast, practical defense and vaccination for deep learning using JPEG compression. In *ACM SIGKDD International Conference on Knowledge Discovery & Data Mining*, 2018.
- [11] Steven Diamond, Vincent Sitzmann, Stephen Boyd, Gordon Wetzstein, and Felix Heide. Dirty pixels: Optimizing image classification architectures for raw sensor data. *arXiv preprint arXiv:1701.06487*, 2017.
- [12] Samuel Dodge and Lina Karam. Understanding how image quality affects deep neural networks. In *IEEE International Conference on Quality of Multimedia Experience (QoMEX)*, 2016.
- [13] Yoav Freund and Robert E Schapire. A decision-theoretic generalization of on-line learning and an application to boosting. *Journal of computer and system sciences*, 55(1), 1997.
- [14] Zhitao Gong, Wenlu Wang, and Wei-Shinn Ku. Adversarial and clean data are not twins. *arXiv preprint arXiv:1704.04960*, 2017.
- [15] Kathrin Grosse, Praveen Manoharan, Nicolas Papernot, Michael Backes, and Patrick McDaniel. On the (statistical) detection of adversarial examples. *arXiv preprint arXiv:1702.06280*, 2017.
- [16] Chuan Guo, Mayank Rana, Moustapha Cisse, and Laurens van der Maaten. Countering adversarial images using input transformations. In *ICLR*, 2018.
- [17] Puneet Gupta and Esa Rahtu. Ciidefence: Defeating adversarial attacks by fusing class-specific image inpainting and image denoising. In *Proceedings of the IEEE International Conference on Computer Vision*, pages 6708–6717, 2019.
- [18] Kaiming He, Xiangyu Zhang, Shaoqing Ren, and Jian Sun. Deep residual learning for image recognition. In *CVPR*, 2016.
- [19] Warren He, James Wei, Xinyun Chen, Nicholas Carlini, and Dawn Song. Adversarial example defenses: Ensembles of weak defenses are not strong. In *USENIX Workshop on Offensive Technologies*, 2017.
- [20] Diederik P Kingma and Jimmy Ba. Adam: A method for stochastic optimization. In *ICLR*, 2015.
- [21] Xin Li and Fuxin Li. Adversarial examples detection in deep networks with convolutional filter statistics. In *ICCV*, 2017.
- [22] Fangzhou Liao, Ming Liang, Yinpeng Dong, Tianyu Pang, Jun Zhu, and Xiaolin Hu. Defense against adversarial attacks using high-level representation guided denoiser. In *CVPR*, 2018.
- [23] Shiqing Ma, Yingqi Liu, Guanhong Tao, Wen-Chuan Lee, and Xiangyu Zhang. NIC: Detecting adversarial samples with neural network invariant checking. In *Network and Distributed System Security Symposium (NDSS)*, 2019.
- [24] Aleksander Madry, Aleksandar Makelov, Ludwig Schmidt, Dimitris Tsipras, and Adrian Vladu. Towards deep learning models resistant to adversarial attacks. In *ICLR*, 2018.
- [25] Julien Mairal, Michael Elad, and Guillermo Sapiro. Sparse representation for color image restoration. *IEEE Transactions on image processing*, 17(1), 2007.
- [26] Dongyu Meng and Hao Chen. MagNet: a two-pronged defense against adversarial examples. In *ACM SIGSAC Conference on Computer and Communications Security (CCS)*, 2017.
- [27] Jan Hendrik Metzen, Tim Genewein, Volker Fischer, and Bastian Bischoff. On detecting adversarial perturbations. In *ICLR*, 2017.
- [28] Seyed-Mohsen Moosavi-Dezfooli, Alhussein Fawzi, and Pascal Frossard. DeepFool: a simple and accurate method to fool deep neural networks. In *CVPR*, 2016.
- [29] Maria-Irina Nicolae, Mathieu Sinn, Minh Ngoc Tran, Beat Buesser, Amrisha Rawat, Martin Wistuba, Valentina Zantedeschi, Nathalie Baracaldo, Bryant Chen, Heiko Ludwig, Ian Molloy, and Ben Edwards. Adversarial robustness toolbox v1.0.1. <https://github.com/IBM/adversarial-robustness-toolbox/blob/master/art/attacks/carlini.py>, 2018.
- [30] Nicolas Papernot, Patrick McDaniel, Xi Wu, Somesh Jha, and Ananthram Swami. Distillation as a defense to adversarial perturbations against deep neural networks. In *IEEE Symposium on Security and Privacy (SP)*, 2016.
- [31] Aaditya Prakash, Nick Moran, Solomon Garber, Antonella DiLillo, and James Storer. Deflecting adversarial attacks with pixel deflection. In *CVPR*, 2018.
- [32] Aaditya Prakash, Nick Moran, Solomon Garber, Antonella DiLillo, and James Storer. Protecting jpeg images against adversarial attacks. In *2018 Data Compression Conference*, pages 137–146. IEEE, 2018.
- [33] Jonas Rauber, Wieland Brendel, and Matthias Bethge. Foolbox: A Python toolbox to benchmark the robustness of machine learning models. *arXiv preprint arXiv:1707.04131*, 2017.
- [34] Jianhong Shen and Tony F Chan. Mathematical models for local nontexture inpaintings. *SIAM Journal on Applied Mathematics*, 62(3), 2002.
- [35] Alexandru Telea. An image inpainting technique based on the fast marching method. *Journal of Graphics Tools*, 9(1), 2004.
- [36] Shixin Tian, Guolei Yang, and Ying Cai. Detecting adversarial examples through image transformation. In *AAAI Conference on Artificial Intelligence*, 2018.
- [37] Weilin Xu, David Evans, and Yanjun Qi. Feature squeezing: Detecting adversarial examples in deep neural networks. In *Network and Distributed System Security Symposium (NDSS)*, 2018.

- [38] Stephan Zheng, Yang Song, Thomas Leung, and Ian Goodfellow. Improving the robustness of deep neural networks via stability training. In *CVPR*, 2016.
- [39] Fei Zuo, Bokai Yang, Xiaopeng Li, Lannan Luo, and Qiang Zeng. Exploiting the inherent limitation of L_0 adversarial examples. In *International Symposium on Research in Attacks, Intrusions and Defenses (RAID)*, 2019.